

1 **Strength in Numbers: Insights from Initial-condition Large Ensembles with Multiple Earth**
2 **System Models and Future Prospects**

4 US CLIVAR Working Group on Large Ensembles

5 [C. Deser*, F. Lehner, K.B. Rodgers, T. Ault, T.L. Delworth, P.N. DiNezio, A. Fiore, C. Frankignoul,
6 J. C. Fyfe, D.E. Horton, J.E. Kay, R. Knutti, N.S. Lovenduski, J. Marotzke, K.A. McKinnon, S.
7 Minobe, J. Randerson, J.A. Screen, I.R. Simpson and M. Ting]

9 Perspective in *Nature Climate Change*

10 Submitted June 21, 2019; Revised November 27, 2019

12 *Corresponding author: Dr. Clara Deser, National Center for Atmospheric Research, Boulder CO
13 cdeser@ucar.edu

15 **1. Abstract**

16 Internal variability in the climate system confounds assessment of human-induced climate
17 change and imposes irreducible limits on the accuracy of climate change projections, especially
18 at regional and decadal scales. A new collection of initial-condition large ensembles performed
19 with seven Earth System Models under historical and future radiative forcing scenarios provides
20 new insights into uncertainties due to internal variability vs. model differences. These data
21 enhance the assessment of climate change risks including extreme events. In addition, they offer
22 a powerful testbed for new methodologies aimed at separating forced signals from internal
23 variability in the observational record. Opportunities and challenges confronting the design and
24 dissemination of future large ensembles, including consideration of increased spatial resolution
25 and model complexity along with emerging earth system applications, are discussed.

27 **2. Introduction**

28 Identifying anthropogenic influences on weather and climate amidst the background of internal
29 variability, and providing projections of future changes, are central scientific challenges with
30 practical implications^{1–6}. Since the inception of the Coupled Model Intercomparison Project
31 (CMIP) nearly two decades ago, substantial progress has been made on quantifying sources of
32 uncertainty in climate projections (e.g., ref^{7–9}). However, such multimodel archives confound
33 uncertainties arising from differences in model formulation (i.e., structural uncertainty) with
34 those generated by internal variability (variability arising from processes intrinsic to the coupled
35 ocean-atmosphere-land-biosphere-cryosphere system). This distinction is important, because
36 the former is potentially reducible as models improve, whereas the latter is an intrinsic property
37 of each model and is largely irreducible after the memory of initial conditions is lost, typically
38 after less than a few years over land¹⁰. This key distinction is often not widely appreciated and
39 communicated to stakeholder groups¹¹. Indeed, internal variability accounts for approximately
40 half of the inter-model spread within the CMIP archive for projected changes in near surface air
41 temperature, precipitation and runoff across North America and Europe over the next 50 years
42 ^{5,8,9,12–14}.

43

44 One way to isolate the contribution of uncertainty due to internal variability is to perform an
45 ensemble of simulations with a single fully-coupled global climate model under a particular
46 radiative forcing scenario, applying perturbations to the initial conditions of each member in
47 order to create diverging weather and climate trajectories, causing ensemble spread (e.g.,
48 ref^{12,15-17}). Since the resulting sequences of unpredictable internal variability are randomly
49 phased between the individual ensemble members, the forced response can be estimated by
50 averaging over a sufficient number of members. The definition of “sufficient” depends on the
51 quantity of interest, location, spatial scale, temporal scale, and time horizon, often on the order
52 of 10-100 members (e.g., ref¹²). Such “initial-condition Large Ensembles” conducted with fully-
53 coupled global models (hereafter referred to as “LEs”) are a relatively new development in
54 climate sciences, with the first efforts employing CMIP3-era models^{12,18}.

55

56 The past few years have witnessed an explosion of LEs with newer-generation CMIP5-class Earth
57 System Models (ESMs; Table 1). Each LE required substantial high performance computing
58 resources to produce, and generated hundreds of terabytes of output. For example, the CESM1
59 LE used 21 million CPU hours and produced over 600 terabytes of model output (for comparison,
60 the entire CESM1 contribution to CMIP5 was 170 terabytes). Making these “big data” projects
61 accessible to a wide range of users is challenging. Yet, their ease-of-use for different types of
62 analysis work-flows has a substantial impact on the scientific value gained from their production.
63 A case in point is the NCAR CESM1-LE Project¹⁹, which from the outset had an explicit goal of
64 serving a broad research community by responding to user needs to provide easy access to the
65 output and stable on-disk access. This project has resulted in more than 750 peer-reviewed
66 studies to date, with approximately 400,000 data files downloaded from spinning disk. Remaining
67 nimble to new workflows and users is important, as is following the recommended “big data”
68 practice of “bringing your analysis to your data”. Following these principles, the CESM1-LE was
69 made freely available as a public dataset on the Amazon Web Services cloud in autumn 2019.
70 Access on the commercial cloud demonstrates strong interest in LEs from industry and scientific
71 communities well beyond typical climate researchers that have historically used climate models.
72 Such scrutiny and widespread use attests to the enormous value of LEs for a range of applications:
73 truly a “sea-change” for climate and related sciences.

74

75 **3. Strength in Numbers: a Multi-Model Large Ensemble Archive**

76 While a single model LE has enormous utility, a multimodel collection of LEs can be leveraged for
77 robust comparison of the forced response on regional/decadal scales across models, as well as
78 of the characteristics of internal variability across models. It can also advance model evaluation
79 by providing more complete information on biases in internal variability vs. those in the forced
80 response. Unlike CMIP, a multimodel archive of LEs allows for direct separation of projection
81 uncertainty into a structural component due to model differences and an internal variability
82 component. Despite these advantages, most analyses to date have been limited to one or at most
83 two LEs (with a few exceptions, e.g., refs^{20,21}), in part because of the burdensome task of
84 accessing large volumes of data from disparate sources. To fill this gap, we have produced a
85 centralized data repository of LEs conducted with seven different CMIP5-class ESMs under
86 historical and future emissions scenarios (hereafter referred to as the “Multi-Model Large
87 Ensemble Archive” or MMLEA; Table 1). This repository includes gridded fields of key variables at

88 daily and monthly resolution, and is easily accessible via the NCAR Climate Data Gateway
89 ([https://www.earthsystemgrid.org/dataset/ucar.cgd.ccsm4.CLIVAR LE.html](https://www.earthsystemgrid.org/dataset/ucar.cgd.ccsm4.CLIVAR_LE.html)).

90
91 This Perspective seeks to illustrate some of the new insights that can be gained from the MMLEA,
92 with the aim of widening its usage and stimulating new research directions including emerging
93 Earth system applications. We also look to the future of initial-condition LEs, in particular the
94 opportunities and challenges that confront their design and facilitate their accessibility to the
95 broad user community. In this regard, we offer a path forward that balances demands for
96 increased spatial resolution and model complexity against ensemble size. We encourage future
97 phases of CMIP to take on a greater role in the design of LE simulations and in coordinating their
98 data storage and access.
99

100 **4. New insights on separating sources of uncertainties**

101 Individual LEs have been crucial to show that internal variability needs to be considered alongside
102 forced trends in past and future climate change at continental and smaller spatial scales (i.e.,
103 refs^{10,12,14,19,22–30}). The MMLEA expands on this view by providing new insights on the relative
104 roles of internal variability and model structural differences -- two sources of projection
105 uncertainty in addition to radiative forcing scenario. The MMLEA shows that both factors can
106 play a first-order role in the magnitude and pattern of warming at continental scales. As an
107 example, Fig. 1 show the distributions of trends in North American air temperatures over the last
108 60 years from each of the seven LEs (Methods). While they all encompass the observed trend
109 value, they clearly differ in the strength of the forced trend (given by the ensemble mean) and in
110 the shape and width of the distribution of trends, which emerges due to the influence of internal
111 variability. This information on model-dependence of both the forced trend and the range of
112 trends due to internal variability is unique to the MMLEA, and could not have been deduced
113 directly from the CMIP archives. It is important to note that a LE that is centered on the single
114 observed trend value does not constitute evidence that this particular model is more realistic
115 than any other model (see further discussion in Section 6).

116
117 The distribution of North American temperature trends based on the 40 models in the CMIP5
118 archive (Methods) is only slightly wider than that based on an individual LE, and is due to both
119 model differences and internal variability (see gray shaded PDF in Fig. 1). Moreover, the MMLEA
120 as a whole spans a wider range than CMIP5, suggesting that CMIP5 under-samples internal
121 variability at regional scales. This highlights the importance of evaluating the realism of models'
122 internal variability of trends, since a model with unrealistically large trend variability (i.e., a broad
123 distribution) can encompass the observed trend for the wrong reason and would also inflate
124 uncertainty in future projections. Approaches to address this challenge are discussed in Section
125 6.
126

127 Just as North American temperature trends vary across the individual members of a LE, the
128 geographical pattern of trends can also be strikingly different (row of maps at the bottom of Fig.
129 1). This can confound comparisons of individual simulations from different models and lead to
130 erroneous interpretations, since internal variability might be mistaken for structural differences.
131 With enough members, the spatial pattern of the forced response emerges for each model,

132 allowing for a direct comparison between models. Models may show similar forced patterns of
133 poleward-amplified warming but different overall amplitudes (top left and right maps in Fig. 1),
134 a conclusion that would have been difficult to discern without an MMLEA. Similar issues confront
135 the study of trends observed in the real world (middle map in the top row of Fig. 1), since these
136 are also just one realization of many that could have happened (see Section 6).

137
138 Quantifying model uncertainty requires knowledge of the forced response in each model – but
139 most models in past and current CMIPs do not have enough ensemble members to allow for a
140 robust estimate of its forced response. Instead, low-frequency statistical fits to a single ensemble
141 member are often used to estimate the forced response (e.g., refs^{8,9}). Consequently, internal
142 variability has to be estimated either from the residual of this fit or from long pre-industrial
143 control simulations. From these approaches it is often not easy or possible to robustly estimate
144 systematic changes to internal variability under increasing radiative forcing. The availability of an
145 MMLEA circumvents these limitations and assumptions. More importantly, it allows one to
146 separate the sources of uncertainty at smaller spatial and temporal scales, and for quantities that
147 are notoriously variable such as precipitation and extremes.

148
149 **5. Decision-making and risk assessment in a highly variable climate system**
150 LEs are increasingly proving their utility in the context of real-world decision-making³¹ where full
151 assessment of changing climate risks is needed, including variability and extremes. In particular,
152 discerning changes in variability and extremes requires large sample sizes^{32–36}, the hallmark of
153 LEs. Moreover, the MMLEA is critical for evaluating the extent to which projected changes in
154 variability and extremes are model dependent.

155
156 The Upper Colorado River basin – which feeds the largest reservoirs in the US – is a clear example
157 of where changes in mean and variability can produce a wide range of climate risks for water
158 managers. This basin is located at a latitude where projected changes in precipitation are
159 notoriously uncertain – the transition zone between the expected drying in the subtropics and
160 the wetting at high latitudes^{2,37–39}. The MMLEA shows divergent outcomes regarding how
161 decadal mean precipitation will change in this region under a high-emissions scenario (Fig. 2a).
162 However, decadal variability of precipitation is projected to increase, on average by about 10%
163 of the magnitude of the forced change (Fig. 2b). This result by itself suggests a heightened hazard
164 of prolonged droughts and pluvials, and could, in the absence of consistent projections of
165 changes in the mean, provide useful information for refining water management strategies.

166
167 To illustrate the challenge of projecting extreme events, we use an example of daily summer heat
168 extremes for a location in the south-central United States centered on Dallas, Texas (Methods).
169 As expected under global warming, daily July heat extremes at Dallas are projected to increase
170 over the 21st century; however, their evolution is far from monotonic in any single ensemble
171 member, and their rate and degree of increase varies considerably across different realizations
172 of future internal variability in the same model (Fig. 3a). For instance, historical daily heat records
173 could be broken almost continuously starting in the late 2060s, or their occurrence could be more
174 punctuated, with some decades even as late as the 2090s spared from any days of record heat,
175 depending on how internal variability happens to unfold (Fig. 3a). The variety of temporal

176 expressions of historical heat extreme exceedances across the different members of an LE should
177 be a cautionary note on the enormous impact of internal variability on rare events (see also refs
178 30 and 31). Results also differ between models, as differences in the amount of warming and in
179 the magnitude of variability combine into an uncertain future risk of exceeding a given threshold
180 (Fig. 3b). Validating not only a model's climatology or mean trend, but also its variability, emerges
181 thus again as an important step when investigating, and ultimately constraining, future
182 projections, in this case of extreme events⁴⁰.
183

184 Attribution-focused large ensembles differ from those in the MMLEA in that they often rely on
185 regional, or high resolution global, atmosphere-land models in order to capture the small spatial
186 scales of specific extreme events^{34–36,41,42} and may prescribe additional boundary conditions such
187 as the large-scale atmospheric circulation^{43,44}. Nevertheless, these types of ensemble highlight
188 the large number of simulations required to identify significant shifts in the probability of certain
189 events. We note that LEs can also serve these alternate types of ensemble by providing lateral
190 boundary conditions to more specialized regional climate models⁴⁵, and oceanic boundary
191 conditions to higher-resolution global atmosphere-land models.
192

193 **6. Multi-model LEs as methodological testbeds with application to an 'Observational' LE**

194 Another key usage of LEs is to test methods suitable for application to the observational record,
195 for example those aimed at separating the signals of internal variability and forced climate
196 change from a single realization (e.g., refs^{28,29,46–50}). Using observations alone, it is difficult to
197 assess the skill of such separation methods due to lack of true knowledge of the observed forced
198 response or the full range of variability, including extremes. However, separation methods can
199 be evaluated by applying the methodology to each LE ensemble member individually and
200 comparing the results to the model's forced response, estimated from the ensemble mean of the
201 LE (Fig. 4). Application to the MMLEA will identify if the validation has a strong dependence on
202 model structure.
203

204 An additional testbed application of model LEs is the development of surrogate realizations of
205 internal variability based on observations (Fig. 4). Although one cannot replay the "tape of
206 history"⁵¹ with an initial-condition perturbation in the real world, the single observed trajectory
207 is only one of many that could have plausibly occurred (under the same boundary conditions and
208 forcing), had a different sequence of internal variability unfolded. This is the underlying premise
209 of LEs: that internal variability can play out with a different (and largely unpredictable)
210 chronology, thereby creating uncertainty in the estimate of trends that are calculated over a
211 finite time interval. Can the sample of internal variability contained within the observational
212 record be used to generate surrogate realizations whose statistical characteristics are largely
213 unchanged, but whose temporal sequences are altered? If so, an observationally-based LE can
214 be developed, wherein these surrogates are added to an estimate of the forced response
215 (derived from models or empirical methods applied to observations) to produce an
216 observationally-constrained range of outcomes (Fig. 4).
217

218 Several methods for generating surrogate realizations that aim to preserve the temporal²⁵ and
219 spatio-temporal characteristics of observed internal variability have been proposed^{46,52–57}. To

220 date, these techniques have been applied to terrestrial temperature and precipitation^{25,46}, sea
221 level pressure⁴⁶, and sea-surface temperature^{52,54}. These methods interact in two important ways
222 with model LEs. First, model LEs can be used as methodological testbeds to ensure that the
223 statistical ensembles have the desired properties (Fig. 4). Second, after the statistical ensembles
224 are validated, they can then be used to validate the model LEs. We demonstrate this interplay
225 with an example from the “Observational Large Ensemble” (Obs-LE) developed by ref⁴⁶
226 (Methods).

227

228 Analogous to the approach mentioned above for estimating the forced trend, the Obs-LE
229 methodology can be cleanly tested in the context of a model LE by creating a statistical ensemble
230 based on a single member of the model LE, and assessing whether the spread of the statistical
231 ensemble is consistent with that of the remaining ensemble members. This procedure can then
232 be repeated for each ensemble member, and the resulting information pooled together to
233 provide a robust estimate of the accuracy of the methodology (Fig. 4). In the case of variability
234 of annual temperature trends over the past 50 years on land, the fractional error of the Obs-LE
235 methodology is generally less than 20% over most of the globe, with slightly larger errors in
236 certain regions of the tropics (Fig. 5a). Assuming the properties of the real world are not
237 drastically different from those of the model, this indicates that applying the same approach to
238 generate a statistical ensemble from the single realization of the real world is valid.

239

240 Having validated the Obs-LE approach, one can then assess the realism of internal variability
241 simulated by each model LE by comparison with the Obs-LE. For the case of the CESM1-LE, the
242 model overestimates variability of 50-year temperature trends by up to 50% in parts of western
243 North America and northern Eurasia, and up to 100% in areas of high terrain in the tropics (Fig.
244 5b). These model biases in variability are larger than the error of the Obs-LE methodology,
245 indicating they are true model biases. Similar results are found for precipitation trend variability,
246 which exhibits regions of both significant underestimation and overestimation in the CESM1-LE⁴⁶.

247

248 One can also apply the Obs- LE to evaluate the simulated distributions of temperature trends at
249 specific locations. For example, the simulated temperature trend distributions for Dallas, Texas
250 in the CESM1 and MPI LEs narrow considerably when the Obs-LE is used to estimate the internal
251 variability (inset to Fig. 5b), consistent with the models’ significant overestimation of variability
252 at this location. This brings the observed trend closer to the lower tail of the distributions. It is
253 worth emphasizing that without an observationally-based LE, it would not have been possible to
254 assess the width of the models’ temperature trend distributions, with important implications for
255 constraining future projections.

256

257 An important future challenge for the LE community is to develop effective means to evaluate
258 and benchmark the internal variability generated by model LEs. Meeting this challenge requires
259 taking advantage of historical and paleoclimate records, and developing suitable statistical
260 emulation methods to construct observationally-based LEs for other components of the climate
261 system. Statistical emulation of internal variability may also be advantageous in the context of
262 ESMs when the cost of conducting a sufficiently large LE is prohibitive, for example, in the case
263 of models with increased spatial resolution and/or complexity (discussed further below). These

264 statistical emulation methods will need to take into account any projected changes in internal
265 variability⁵⁸.

266

267 **7. Looking to the future of initial-condition LEs**

268 ***a) Considerations on LE design***

269 The existing LEs have been designed and created independently, with different choices of time
270 period, radiative forcing scenario, number of members and method of initialization (Table 1). In
271 addition, they employ different protocols for data output, storage and access. These differences
272 must be considered when comparing LEs across models, as each has ramifications.

273

274 *Initialization*

275 In some LEs, the initial conditions are created by introducing minuscule (at the level of round-off
276 error or 10^{-14} K) perturbations into the atmosphere only (“micro perturbation”¹⁵). The rapid
277 growth of atmospheric perturbations makes this technique well suited for studies involving
278 atmospheric variability and trends. However, for phenomena with long persistence involving
279 oceanic or terrestrial processes, such as sea level, ocean heat content, biogeochemistry, and soil
280 moisture, it may be more desirable to start each member from completely different initial
281 conditions in the ocean and other components (“macro perturbations”) to more fully sample
282 different possible climate trajectories. Macro perturbations can increase the ensemble utility,
283 but can introduce complications related to subsurface ocean drift in the control simulation that
284 can influence ocean initial conditions, and thus require long and quasi-equilibrated control
285 simulations to choose initial conditions from⁵⁹. A combination of micro and macro perturbations
286 could have the most scientific benefit, but the issue of ensemble initialization clearly needs close
287 examination, and potential coordination between multiple LE projects.

288

289 *Length of simulation and ensemble size*

290 For a given amount of computer time, a choice has to be made between the length of the
291 simulations versus the number of ensemble members. For example, is it better (for some
292 purposes) to have a 100-member ensemble covering the period 1981-2040 or a 50-member
293 ensemble extending over 1981-2100? Furthermore, if higher spatial-resolution is critical, such as
294 for the simulation of some climate extremes, this usually comes at the expense of the total
295 number of ensemble members that can be run. The optimal balance between ensemble size and
296 spatial resolution will depend on the specific purposes of the LE (see also ref⁶⁰).

297

298 *Radiative forcing scenario*

299 The choice of forcing scenario may impact the characteristics of internal variability. Is it better to
300 run more members using a single choice of a forcing scenario, or multiple smaller ensembles with
301 differing scenarios? Even single scenarios are normally comprised of individual forcing
302 components (e.g. greenhouse gases and aerosols), and for the important but otherwise elusive
303 goal of attribution, the use of ensembles with a single radiative forcing (for example, only
304 changing aerosols) can provide critical insights into the mechanistic drivers^{61,62}.

305

306 *Data output, storage and access*

307 As the scientific foci of LE applications expand to encompass a broader set of resolved timescales
308 (diurnal to centuries), practical limitations arise not only from the computational burden but also
309 from the storage requirements to maintain and make available hundreds of terabytes of data for
310 analysis. At present, some LEs only provide monthly-averaged output, while others provide daily
311 averages but only for select fields. In general, practical storage limitations require a compromise
312 between ensemble size and choice of output fields. Model fields can also be in formats that are
313 not intuitive to use for users, limiting accessibility. Careful consideration should be given not only
314 to data storage, enabling workflows that bring analysis to the data, but also to format. We
315 recommend single variable time series. We also recommend that given that ocean model grids
316 are in general non-uniform, meeting growing user demand should also prompt modeling centers
317 to provide some LE output interpolated onto conventional grid structures and/or the tools
318 necessary to accomplish the regridding.
319

320 ***b) Accommodating increased model complexity and spatial resolution***

321 High resolution regional climate projections can also benefit from the “strength in numbers” of
322 MMLEs. As mentioned above, dynamical downscaling techniques can help resolve processes at
323 spatial scales that are not well resolved by global ESMs, and statistical downscaling can be used
324 to map from large to small spatial scales. Currently, such efforts are still limited by the classic
325 trade-off between ensemble size and spatial resolution, with most studies performing
326 downscaling from only one LE and for only part of the globe (e.g., ref^{45,63}). An alternative
327 approach is to select events of interest from an MMLE, such as particular extremes (e.g., ref⁶⁴) or
328 ENSO events (e.g., refs^{65,66}), and perform regional downscaling to better understand their
329 dynamics and predictability. Finally, we note that other ensemble methodologies could benefit
330 from incorporating the information from initial-condition LEs into their design. For example,
331 perturbed parameter ensembles (ref⁶⁷) can be a useful approach to probe the uncertainties
332 arising from the lack of constraint on uncertain model parameters. However, they will only serve
333 their purpose if, for each parameter combination, a sufficient number of ensemble members is
334 performed to allow for the isolation of that parameter influence amidst the internal variability.
335

336 The above findings and discussion provide a powerful argument for the importance and utility of
337 LEs with multiple ESMs for the climate science and climate impacts communities. However, the
338 ever-growing need for more ensembles using higher spatial resolution⁶⁸ and more
339 comprehensive representations of the Earth System poses an enormous computational
340 challenge, especially balanced against other demands for resources in the use and continued
341 development of climate models, such as refining spatial resolution, improving numerical
342 methods, incorporating more realistic and comprehensive physical and biophysical processes,
343 and saving ever-expanding volumes of data.
344

345 One potential pathway out of this dilemma is to take a two-pronged approach. The first is the
346 continuation of the current path, creating and extending large ensembles with current and newly
347 developed models. These data sets have yet to be fully mined and will continue to provide critical
348 insights. The second pathway is to focus on developing new techniques that can create efficient
349 statistical descriptions of the complete distribution from large ensembles, including extreme
350 events^{46,55-57}. These efficient emulation techniques would allow the generation of arbitrarily

351 large ensembles at a fraction of the computational cost associated with the traditional large
352 ensembles. This would require a focused effort to develop and validate these new techniques,
353 taking advantage of existing large ensembles as testbeds for the fidelity of the new techniques.
354 If this capability were successfully developed, computational resources could be focused on
355 limited sets of ensembles employing very high resolution, comprehensive Earth System Models
356 – the types of models that many applications are now demanding. After training on the new
357 “super” data sets produced by these models, the goal would be for the new emulation techniques
358 to allow the efficient production of arbitrarily large ensembles that are indistinguishable from
359 ensembles from the underlying models. One could envision a paradigm in which the required
360 ensemble size for the most comprehensive high-resolution models would be the smallest number
361 that is able to both (a) satisfactorily characterize the model’s response to radiative forcing
362 changes, and (b) provide a sufficient data set for training the emulators. A community discussion
363 on how to optimize the scientific return on computational investment from LEs while continuing
364 to advance climate modeling along multiple pathways would be of great value.
365

366 **8. Emerging Earth System Applications**

367 Several communities have developed approaches to balance the trade-offs between increasing
368 complexity and their computational costs. In some cases, raw, bias-corrected or downscaled
369 meteorological fields archived from climate models are used to drive offline models that include
370 more complexity (e.g., atmospheric composition, air quality, hydrologic models) or to conduct
371 impact assessments (health burdens, economic valuations, reservoir operations)^{69–71}. While
372 these trade-offs will continue as next-generation developments in atmospheric chemistry,
373 hydrology, resource management, and integrated assessment approaches continue to expand in
374 complexity, the development of LEs and MMLEs represent a new research frontier for these
375 applications. Below, we highlight some climate subfields where advances should be possible with
376 the existing climate-focused MMLEs as well as examples where LEs with more complexity are
377 already advancing scientific knowledge (ocean biogeochemistry) and where a single LE has yet to
378 be generated (atmospheric chemistry). We also discuss applications of LEs that apply broadly
379 across the Earth System.
380

381 Several stakeholder communities may be well-positioned to immediately tap the power of the
382 existing MMLEs. By providing large sample sizes, LEs enable construction of probabilistic
383 frameworks for risk assessment. For example, the existing MMLE archive may offer opportunities
384 to flesh out the tails of probability distributions of future public health burdens, crop yields, or
385 fisheries catch. That is, to the extent that the probabilistic occurrence of complex extreme
386 phenomena can be assessed using commonly simulated meteorological variables (e.g., refs^{72–74}),
387 a MMLEA offers the ability to independently assess the contributions role of internal variability,
388 anthropogenic climate change, and model uncertainty to projected changes. By design, such
389 statistical approaches inherently assume the key drivers are meteorological and neglect
390 feedbacks with, e.g. the biosphere, that can be included in more specialized ESMs, e.g., Coupled
391 Chemistry Models. The power of LEs – even without additional complexity – as tools to
392 investigate mean state biases⁷⁵, extreme events and their impacts on ecosystems, food security,
393 and public health remains largely unexplored.
394

395 A growing collection of ocean biogeochemistry studies have highlighted the utility of single-
396 model LEs for quantifying the time of emergence for important biogeochemical variables such as
397 air-sea carbon dioxide fluxes²³, interior ocean oxygen concentration²⁴, marine ecosystem
398 drivers⁷⁶, and interior ocean carbon cycling⁷⁷. Additional work with single-model LEs has been
399 used to quantify the role of internal variability in projection uncertainty for air-sea carbon dioxide
400 fluxes⁷⁸ and ecosystem stressors⁷⁹, to identify avoidable impacts in the future evolution of
401 phytoplankton net primary production with anthropogenic climate change⁸⁰, and to quantify the
402 number of ensemble members needed to detect decadal trends in air-sea CO₂ flux⁸¹. While
403 changes in phenology under future climate perturbations have been examined in a single LE for
404 a terrestrial ecosystem⁸², we anticipate much broader future applications to both terrestrial and
405 oceanic ecosystems as there are clear implications for ecosystem behavior and resource
406 management.

407
408 Due to the computational expense of simulating atmospheric chemistry within fully coupled
409 ESMs, atmospheric composition and air quality have not yet been explored within a single LE,
410 even though it is well established that atmospheric constituents vary with weather and climate.
411 Changes in pollution events and public health burdens have been investigated through dynamical
412 downscaling (e.g., refs^{70,83}) of a limited period from global climate models, or directly from coarse
413 resolution global chemistry-climate models (e.g., ref⁸⁴). To date, these projections of future
414 composition and air quality have not sufficiently separated internal variability from the forced
415 signal as they rely on small ensembles from a single model (e.g., refs^{71,85}) or multi-model time-
416 slice ensembles (e.g., refs^{86,87}). Nevertheless, a small ensemble from one chemistry-climate
417 model demonstrates the need to account for internal variability when detecting future changes
418 in air quality (or, by extension, atmospheric composition) resulting from anthropogenic climate
419 and emission changes^{88,89}. A single LE with full atmospheric chemistry would enable pursuit of
420 new research questions paralleling those tackled within the climate community. The future
421 development of MMLEs with full atmospheric chemistry would enable exploration of model
422 structural uncertainty separately from internal variability.

423
424 While LEs alone enable one to quantify variations in some variable of interest, in some
425 applications, a set of companion simulations further enhance their utility for decision-
426 making. For example, air quality planners would like to understand not just the role of climate
427 change and variability, but also the influence of air pollutant emission pathways on future
428 projections. One path to address this need could be to follow the approach discussed above for
429 extreme events in which high-frequency time fields are saved for use in dynamical downscaling.
430 Archiving fields needed to drive air quality models would open up the possibility for multiple
431 sensitivity simulations focused on a target time period and region, or even single pollution event,
432 of interest. Another example involves resource managers who are interested in near-term
433 prediction (1-10 year time scales). The CESM-LE, when paired with the CESM Decadal Prediction
434 Large Ensemble (CESM-DPLE⁹⁰) has been shown to provide a significant advance in deepening
435 our understanding of near-term predictability and its origin⁹⁰.

436
437 Part of the promise offered by LEs is in informing optimization of observing system design and
438 duration. For example, in fields where observations are notoriously sparse (e.g., ocean

439 biogeochemistry), LEs offer a powerful approach to assess where future measurements can most
440 readily detect trends driven by anthropogenic forcing (e.g., where signal-to-noise is largest). In
441 turn, LEs are useful for interpreting limited observational datasets in the context of internal
442 variability. Internal variability could vary strongly with anthropogenic forcing in non-linear
443 systems, such as ocean carbonate or atmospheric chemistry, but without an LE, this signal is
444 challenging to identify. The development of MMLEs in these fields would further allow
445 investigation of model structural uncertainty separately from internal variability.

446

447 **9. Next steps: Fostering effective LE design and implementation, and incorporating LEs into 448 CMIP7**

449 Enabling discovery and advances for a broad community is key to justifying the substantial human
450 and computing resources required for effective LE projects. Designing LE experiments with useful
451 outputs and bringing diverse workflows to these large datasets is challenging. How do we foster
452 effective LE design and implementation? The experience of this author list in generating and
453 sharing data, including especially the most widely used LE project to date - NCAR CESM1-LE
454 Project¹⁹ - provides several lessons. First, open and free access to useful variables from a wide
455 range of components (ocean, atmosphere, land, ice) is critical. Involvement of a broad
456 community of users at the outset is essential to define the variables to save including their
457 temporal frequency, as well as to determine other aspects of the project such as ensemble size,
458 temporal duration, radiative forcing scenario, and method of initialization. Second, data formats
459 matter. Data should be distributed in a format that is easily ingested into user workflows. The
460 current gold standard data format is single variable time series in a self-documenting format (e.g.,
461 netcdf) on a uniform latitude-longitude grid. Third, documentation matters. Developing well
462 written documentation that enables users to scope out and realize the potential for their
463 applications is necessary. As is well known from CMIP and previous LE efforts, documentation
464 and communication about climate modeling projects requires dedicated human resources.
465 Updates must be continuous, easily accessed, and responsive to user concerns and questions.
466 While easy-to-use data formats and effective documentation will be enough for experienced
467 users, help for new communities who are not the traditional users of climate model output is
468 also needed. Targeted tutorials and example analysis workflows will enable more users to
469 become involved and increase the knowledge gained through the production of LE datasets.
470 Finally, on the computational side, it is necessary to consider not only the computational needs
471 for producing LE data, but also the long-term storage and computational needs to make these
472 data usable, free, and accessible over a long period of time. Long-term data storage and bringing
473 diverse user workflows to the dataset are key. In addition, users should be able to complete off-
474 shoot experiments that build on the foundation of the original LE, something that is only possible
475 if the original code is maintained and distributed publicly and required restart files are provided.
476 Future LE projects should consider the best way to follow the big data mantra of bringing the
477 analysis to the data for a large number of users. Moving away from workflows where individual
478 users download LE datasets to work on their own computers is advised. Identifying efficient
479 storage and workflow options at the onset that will enable LE data to be most efficiently used is
480 essential. Along these lines, the potential of the commercial cloud is certainly worth further
481 exploring, while also being aware of intellectual property, who will pay, and other concerns that
482 may arise. Careful thought and resources to address these above four considerations

483 undoubtedly contributed to the widespread use and success of the CESM1-LE, and are currently
484 informing the design of the next-generation LEs. Experience shows that choices made in the
485 design and implementation of an LE have substantial implications for its scientific utility.

486
487 While much success has been found with LE experiments outside of official CMIP coordination,
488 we recommend increased integration and assessment of LE experiments within CMIP7.
489 Integration of LEs within the next phase of CMIP will characterize internal variability within the
490 context of a large computational experiment already being coordinated and conducted
491 internationally. Incorporating LE design and knowledge into CMIP will directly address challenges
492 noted above with regard to partitioning projection uncertainty into structural and internal
493 variability components. Toward this end, for CMIP7 we recommend that modeling centers have
494 a strategy to incorporate quantification of internal climate variability into all of their MIP
495 contributions. Without such a strategy, we are concerned that internal climate variability will at
496 times continue to be impossible to differentiate from model uncertainty and/or forcing
497 uncertainty. Moving forward, it is critical that the science and policy communities have the
498 capacity to assess internal variability contributions to future climate projections.

499
500 **10. Final remarks**
501 Models form much of the scientific basis for future climate change projections. While the
502 scientific and policy community has focused on projections in the multi-model archives produced
503 by CMIP, CMIP experiments often confound structural uncertainty (i.e., differences in model
504 formulation including physics, parameterizations, resolution, etc.) with internal variability. With
505 the continuously growing MMLE archive introduced here, identifying anthropogenic influences
506 on climate amidst the “noise” of internal variability from a multi-model perspective is finally
507 possible. Scrutiny of this newly available MMLE archive is very much needed, as are answers to
508 the question ‘is a model’s internal variability realistic?’. Separating signal from noise is a grand
509 challenge for all areas of climate science and one that spans all components of the Earth
510 system. Pairing the long-term statistics of the internally driven noise of the climate system
511 provided by LEs with, for example, high resolution simulations, provides a viable path forward to
512 improve understanding of both the statistics and processes underlying extremes. Looking
513 forward, a broad community from computational scientists to stakeholders must be engaged to
514 maximize scientific return on the computing and human investment in new LE efforts.

515
516 **Acknowledgements**
517 We thank the US CLIVAR Office and the US National Science Foundation’s Large Scale Climate
518 Dynamics Program for supporting the activities of the US CLIVAR Working Group on Large
519 Ensembles. We also gratefully acknowledge all of the modeling groups listed in Table 1 for making
520 their Large Ensemble simulations available in the Multi-Model Large Ensemble data repository.
521 We thank the three anonymous reviewers for their constructive comments and suggestions, and
522 Dr. Justin Mankin for inspirational discussions on Large Ensemble use. This Perspective also
523 benefited from discussions that took place at the US CLIVAR Workshop on Large Ensembles held
524 July 2019 in Boulder CO. Some of this material is based upon work supported by the National
525 Center for Atmospheric Research, which is a major facility sponsored by the National Science
526 Foundation under Cooperative Agreement No. 1852977.

1. Solomon, S. *et al.* 2007: Technical Summary. in *Climate change 2007: the physical science basis. Contribution of working group I to the fourth assessment report of the intergovernmental panel on climate change* (2007).
2. IPCC. *Climate Change 2013: The Physical Science Basis. Contribution of Working Group I to the Fifth Assessment Report of the Intergovernmental Panel on Climate Change*. (Cambridge University Press, 2013).
3. Wallace, J. M., Deser, C., Smoliak, B. V. & Phillips, A. S. Attribution of Climate Change in the Presence of Internal Variability. in *Climate Change: Multidecadal and Beyond* (eds. Chang, C.-P., Ghil, M., Latif, M. & Wallace, J. M.) 1–29 (World Scientific, 2015). doi:10.1142/9789814579933_0001
4. Hall, A. Projecting regional change. *Science (80-.).* **346**, (2014).
5. Xie, S. P. *et al.* Towards predictive understanding of regional climate change. *Nature Climate Change* **5**, 921–930 (2015).
6. Stammer, D. *et al.* Science Directions in a Post COP21 World of Transient Climate Change: Enabling Regional to Local Predictions in Support of Reliable Climate Information. *Earth's Futur.* **6**, 1498–1507 (2018).
7. Tebaldi, C. & Knutti, R. The use of the multi-model ensemble in probabilistic climate projections. *Philosophical Transactions of the Royal Society A: Mathematical, Physical and Engineering Sciences* (2007). doi:10.1098/rsta.2007.2076
8. Hawkins, E. & Sutton, R. The potential to narrow uncertainty in regional climate predictions. *Bull. Am. Meteorol. Soc.* **90**, 1095–1107 (2009).
9. Hawkins, E. & Sutton, R. The potential to narrow uncertainty in projections of regional precipitation change. *Clim. Dyn.* **37**, 407–418 (2011).
10. Deser, C., Knutti, R., Solomon, S. & Phillips, A. S. Communication of the role of natural variability in future North American climate. *Nat. Clim. Chang.* **2**, 775–779 (2012).
11. Eyring, V. *et al.* Taking climate model evaluation to the next level. *Nat. Clim. Chang.* **9**, 102–110 (2019).
12. Deser, C., Phillips, A., Bourdette, V. & Teng, H. Uncertainty in climate change projections: The role of internal variability. *Clim. Dyn.* **38**, 527–546 (2012).
13. Kumar, D. & Ganguly, A. R. Intercomparison of model response and internal variability across climate model ensembles. *Clim. Dyn.* **51**, 207–219 (2018).
14. Mankin, J. S., Vivioli, D., Singh, D., Hoekstra, A. Y. & Diffenbaugh, N. S. The potential for snow to supply human water demand in the present and future. *Environ. Res. Lett.* (2015). doi:10.1088/1748-9326/10/11/114016
15. Hawkins, E., Smith, R. S., Gregory, J. M. & Stainforth, D. A. Irreducible uncertainty in near-term climate projections. *Clim. Dyn.* **46**, 3807–3819 (2016).
16. Machete, R. L. & Smith, L. A. Demonstrating the value of larger ensembles in forecasting physical systems. *Tellus, Ser. A Dyn. Meteorol. Oceanogr.* **68**, (2016).
17. Bengtsson, L. & Hodges, K. I. Can an ensemble climate simulation be used to separate climate change signals from internal unforced variability? *Clim. Dyn.* **52**, 3553–3573 (2019).
18. Selten, F. M., Branstator, G. W., Dijkstra, H. A. & Kliphuis, M. Tropical origins for recent

- 571 and future Northern Hemisphere climate change. *Geophys. Res. Lett.* **31**, 4–7 (2004).
- 572 19. Kay, J. E. *et al.* The Community Earth System Model (CESM) Large Ensemble Project: A
573 Community Resource for Studying Climate Change in the Presence of Internal Climate
574 Variability. *Bull. Am. Meteorol. Soc.* 141119125353005 (2014). doi:10.1175/BAMS-D-13-
575 00255.1
- 576 20. Otto, F. E. L. *et al.* Anthropogenic influence on the drivers of the Western Cape drought
577 2015–2017. *Environ. Res. Lett.* **13**, (2018).
- 578 21. Fučkar, N. S. *et al.* On High Precipitation in Mozambique, Zimbabwe and Zambia in
579 February 2018. *Bull. Am. Meteorol. Soc.* (2019).
- 580 22. Diffenbaugh, N. S., Swain, D. L. & Touma, D. Anthropogenic warming has increased
581 drought risk in California. *Proc. Natl. Acad. Sci.* **112**, 3931–3936 (2015).
- 582 23. McKinley, G. A. *et al.* Timescales for detection of trends in the ocean carbon sink. *Nature*
583 **530**, 469–472 (2016).
- 584 24. Long, M. C., Deutsch, C. & Ito, T. Finding forced trends in oceanic oxygen. *Global*
585 *Biogeochem. Cycles* **30**, 381–397 (2016).
- 586 25. Thompson, D. W. J., Barnes, E. A., Deser, C., Foust, W. E. & Phillips, A. S. Quantifying the
587 role of internal climate variability in future climate trends. *J. Clim.* **28**, 6443–6456 (2015).
- 588 26. Lehner, F., Deser, C. & Terray, L. Toward a new estimate of ‘time of emergence’ of
589 anthropogenic warming: Insights from dynamical adjustment and a large initial-condition
590 model ensemble. *J. Clim.* **30**, 7739–7756 (2017).
- 591 27. Dai, A. & Bloecker, C. E. Impacts of internal variability on temperature and precipitation
592 trends in large ensemble simulations by two climate models. *Clim. Dyn.* **52**, 289–306
593 (2019).
- 594 28. Deser, C., Terray, L. & Phillips, A. S. Forced and internal components of winter air
595 temperature trends over North America during the past 50 years: Mechanisms and
596 implications. *J. Clim.* **29**, 2237–2258 (2016).
- 597 29. Sippel, S. *et al.* Uncovering the forced climate response from a single ensemble member
598 using statistical learning. *J. Clim.* (2019). doi:10.1175/JCLI-D-18-0882.1
- 599 30. Swain, D. L., Langenbrunner, B., Neelin, J. D. & Hall, A. Increasing precipitation volatility
600 in twenty-first-century California. *Nat. Clim. Chang.* **8**, 427–433 (2018).
- 601 31. Reclamation, B. of. *Climate Change Adaptation Strategy*. (2016).
- 602 32. *Attribution of Extreme Weather Events in the Context of Climate Change. Attribution of*
603 *Extreme Weather Events in the Context of Climate Change* (National Academies of
604 Sciences, Engineering, and Medicine, 2016). doi:10.17226/21852
- 605 33. Lehner, F., Deser, C. & Sanderson, B. M. Future risk of record-breaking summer
606 temperatures and its mitigation. *Clim. Change* 1–13 (2016). doi:10.1007/s10584-016-
607 1616-2
- 608 34. Mitchell, D. *et al.* Half a degree additional warming , prognosis and projected impacts (HAPPI): background and experimental design. 571–583 (2017). doi:10.5194/gmd-10-
609 571-2017
- 610 35. Otto, F. E. L. *et al.* Climate change increases the probability of heavy rains in Northern
611 England/Southern Scotland like those of storm Desmond - A real-time event attribution
612 revisited. *Environ. Res. Lett.* **13**, (2018).
- 613 36. Ciavarella, A. *et al.* Upgrade of the HadGEM3-A based attribution system to high

- resolution and a new validation framework for probabilistic event attribution. *Weather Clim. Extrem.* **20**, 9–32 (2018).
37. Lehner, F., Deser, C., Simpson, I. R. & Terray, L. Attributing the U.S. Southwest's Recent Shift Into Drier Conditions. *Geophys. Res. Lett.* **45**, 6251–6261 (2018).
38. Seager, R. *et al.* Climate variability and change of mediterranean-type climates. *J. Clim.* **32**, 2887–2915 (2019).
39. Lehner, F. *et al.* The potential to reduce uncertainty in regional runoff projections from climate models. *Nat. Clim. Chang.* **9**, 926–933 (2019).
40. Borodina, A., Fischer, E. M. & Knutti, R. Potential to constrain projections of hot temperature extremes. *J. Clim.* **30**, 9949–9964 (2017).
41. Massey, N. *et al.* Weather@Home-Development and Validation of a Very Large Ensemble Modelling System for Probabilistic Event Attribution. *Q. J. R. Meteorol. Soc.* **141**, 1528–1545 (2015).
42. Mizuta, R. *et al.* Over 5,000 years of ensemble future climate simulations by 60-km global and 20-km regional atmospheric models. *Bull. Am. Meteorol. Soc.* **98**, 1383–1398 (2017).
43. Pall, P. *et al.* Diagnosing conditional anthropogenic contributions to heavy Colorado rainfall in September 2013. *Weather Clim. Extrem.* **17**, 1–6 (2017).
44. Merrifield, A. L. *et al.* Local and non-local land surface influence in European heatwave initial condition ensembles. *Geophys. Res. Lett.* (2019). doi:10.1029/2019GL083945
45. Leduc, M. *et al.* The ClimEx project: A 50-member ensemble of climate change projections at 12-km resolution over Europe and northeastern North America with the Canadian Regional Climate Model (CRCM5). *J. Appl. Meteorol. Climatol.* **58**, 663–693 (2019).
46. McKinnon, K. & Deser, C. Internal variability and regional climate trends in an Observational Large Ensemble. *J. Clim.* (2018).
47. Frankignoul, C., Gastineau, G. & Kwon, Y. O. Estimation of the SST response to anthropogenic and external forcing and its impact on the Atlantic multidecadal oscillation and the Pacific decadal oscillation. *J. Clim.* **30**, 9871–9895 (2017).
48. Wills, R. C., Schneider, T., Hartmann, D. L., Battisti, D. S. & Wallace, J. M. Disentangling Global Warming, Multidecadal Variability, and El Niño in Pacific Temperatures. *Geophys. Res. Lett.* **45**, 2487–2496 (2018).
49. Barnes, E. A., Hurrell, J. W. & Uphoff, I. E. Viewing Forced Climate Patterns Through an AI Lens *Geophysical Research Letters*. (2019). doi:10.1029/2019GL084944
50. Wills, R. C., Battisti, D. S., Armour, K. C., Schneider, T. & Deser, C. Identifying Forced Climate Responses in Climate Model Ensembles and Observations using Pattern Recognition Methods. *J. Clim.*
51. Gould, S. J. *Wonderful Life: The Burgess Shale and the Nature of History*. (W. W. Norton & Co., 1989).
52. Newman, M., Alexander, M. A. & Scott, J. D. An empirical model of tropical ocean dynamics. *Clim. Dyn.* **37**, 1823–1841 (2011).
53. Newman, M., Shin, S. I. & Alexander, M. A. Natural variation in ENSO flavors. *Geophys. Res. Lett.* **38**, 1–7 (2011).
54. Newman, M. An empirical benchmark for decadal forecasts of global surface temperature anomalies. *J. Clim.* **26**, 5260–5269 (2013).

- 659 55. McKinnon, K. A., Poppick, A., Dunn-Sigouin, E. & Deser, C. An 'Observational Large
660 Ensemble' to compare observed and modeled temperature trend uncertainty due to
661 internal variability. *J. Clim.* (2017). doi:10.1175/JCLI-D-16-0905.1
- 662 56. Link, R. *et al.* Fldgen v1.0: An emulator with internal variability and space-Time
663 correlation for Earth system models. *Geosci. Model Dev.* **12**, 1477–1489 (2019).
- 664 57. Castruccio, S., Hu, Z., Sanderson, B., Karspeck, A. & Hammerling, D. Reproducing Internal
665 Variability with Few Ensemble Runs. *J. Clim.* (2019). doi:10.1175/jcli-d-19-0280.1
- 666 58. Poppick, A., McInerney, D. J., Moyer, E. J. & Stein, M. L. Temperatures in transient
667 climates: Improved methods for simulations with evolving temporal covariances. *Ann.
668 Appl. Stat.* **10**, 477–505 (2016).
- 669 59. Maher, N. *et al.* The Max Planck Institute Grand Ensemble – enabling the exploration of
670 climate system variability. *J. Adv. Model. Earth Syst.* (2019). doi:10.1029/2019MS001639
- 671 60. Roberts, M. J. *et al.* The benefits of global high resolution for climate simulation process
672 understanding and the enabling of stakeholder decisions at the regional scale. *Bull. Am.
673 Meteorol. Soc.* **99**, 2341–2359 (2018).
- 674 61. Freychet, N., Tett, S. F. B., Bollasina, M., Wang, K. C. & Hegerl, G. C. The Local Aerosol
675 Emission Effect on Surface Shortwave Radiation and Temperatures. *J. Adv. Model. Earth
676 Syst.* **11**, 806–817 (2019).
- 677 62. Pendergrass, A. G. *et al.* Nonlinear Response of Extreme Precipitation to Warming in
678 CESM1. *Geophys. Res. Lett.* **46**, 10551–10560 (2019).
- 679 63. Aalbers, E. E., Lenderink, G., van Meijgaard, E. & van den Hurk, B. J. J. M. Local-scale
680 changes in mean and heavy precipitation in Western Europe, climate change or internal
681 variability? *Clim. Dyn.* **50**, 4745–4766 (2018).
- 682 64. Gómez-Navarro, J. J. *et al.* Event selection for dynamical downscaling: a neural network
683 approach for physically-constrained precipitation events. *Clim. Dyn.* (2019).
684 doi:10.1007/s00382-019-04818-w
- 685 65. DiNezio, P. N., Deser, C., Okumura, Y. & Karspeck, A. Predictability of 2-year La Niña
686 events in a coupled general circulation model. *Clim. Dyn.* **49**, 4237–4261 (2017).
- 687 66. DiNezio, P. N. *et al.* A 2 Year Forecast for a 60–80% Chance of La Niña in 2017–2018.
688 *Geophys. Res. Lett.* **44**, 11,624–11,635 (2017).
- 689 67. Lambert, F. H. *et al.* Interactions between perturbations to different Earth system
690 components simulated by a fully-coupled climate model. *Clim. Dyn.* **41**, 3055–3072
691 (2013).
- 692 68. Haarsma, R. J. *et al.* High Resolution Model Intercomparison Project (HighResMIP v1.0)
693 for CMIP6. *Geosci. Model Dev.* **9**, 4185–4208 (2016).
- 694 69. Raff, D., Brekke, L., Werner, K., Wood, A. & White, K. *Short-Term Water Management
695 Decisions: User Needs for Improved Climate, Weather, and Hydrologic Information.*
696 (2013).
- 697 70. Hogrefe, C. *et al.* Simulating changes in regional air pollution over the eastern United
698 States due to changes in global and regional climate and emissions. *J. Geophys. Res. D
699 Atmos.* **109**, 1–13 (2004).
- 700 71. Garcia-Menendez, F., Monier, E. & Selin, N. E. The role of natural variability in projections
701 of climate change impacts on U.S. ozone pollution. *Geophys. Res. Lett.* (2017).
702 doi:10.1002/2016GL071565

- 703 72. Horton, D. E., Skinner, C. B., Singh, D. & Diffenbaugh, N. S. Occurrence and persistence of
704 future atmospheric stagnation events. *Nat. Clim. Chang.* **4**, 698–703 (2014).
- 705 73. Shen, L., Mickley, L. J. & Gilleland, E. Impact of increasing heat waves on U.S. ozone
706 episodes in the 2050s: Results from a multimodel analysis using extreme value theory.
707 *Geophys. Res. Lett.* **43**, 4017–4025 (2016).
- 708 74. Yue, X., Mickley, L. J. & Logan, J. A. Projection of wildfire activity in southern California in
709 the mid-twenty-first century. *Clim. Dyn.* **43**, 1973–1991 (2013).
- 710 75. Mulholland, D. P., Haines, K., Sparrow, S. N. & Wallom, D. Climate model forecast biases
711 assessed with a perturbed physics ensemble. *Clim. Dyn.* **49**, 1729–1746 (2017).
- 712 76. Rodgers, K. B., Lin, J. & Frölicher, T. L. Emergence of multiple ocean ecosystem drivers in
713 a large ensemble suite with an Earth system model. *Biogeosciences* **12**, 3301–3320
714 (2015).
- 715 77. Schlunegger, S. *et al.* Emergence of anthropogenic signals in the ocean carbon cycle. *Nat.*
716 *Clim. Chang.* **9**, 719–725 (2019).
- 717 78. Lovenduski, N. S., McKinley, G. A., Fay, A. R., Lindsay, K. & Long, M. C. Partitioning
718 uncertainty in ocean carbon uptake projections: Internal variability, emission scenario,
719 and model structure. *Global Biogeochem. Cycles* **30**, 1276–1287 (2016).
- 720 79. Frölicher, T. L., Rodgers, K. B., Stock, C. A. & Cheung, W. W. L. Sources of uncertainties in
721 21st century projections of potential ocean ecosystem stressors. *Global Biogeochem.*
722 *Cycles* (2016). doi:10.1002/2015GB005338
- 723 80. Krumhardt, K. M., Lovenduski, N. S., Long, M. C. & Lindsay, K. Avoidable impacts of ocean
724 warming on marine primary production: Insights from the CESM ensembles. *Global*
725 *Biogeochem. Cycles* **31**, 114–133 (2017).
- 726 81. Li, H. & Ilyina, T. Current and Future Decadal Trends in the Oceanic Carbon Uptake Are
727 Dominated by Internal Variability. *Geophys. Res. Lett.* **45**, 916–925 (2018).
- 728 82. Labe, Z., Ault, T. & Zurita-Milla, R. Identifying anomalously early spring onsets in the
729 CESM large ensemble project. *Clim. Dyn.* **48**, 3949–3966 (2017).
- 730 83. Fann, N. *et al.* The geographic distribution and economic value of climate change-related
731 ozone health impacts in the United States in 2030. *J. Air Waste Manag. Assoc.* **65**, 570–
732 580 (2015).
- 733 84. Silva, R. A. *et al.* The effect of future ambient air pollution on human premature mortality
734 to 2100 using output from the ACCMIP model ensemble. *Atmos. Chem. Phys.* **16**, 9847–
735 9862 (2016).
- 736 85. Rieder, H. E., Fiore, A. M., Horowitz, L. W. & Naik, V. Projecting policy-relevant metrics
737 for high summertime ozone pollution events over the eastern United States due to
738 climate and emission changes during the 21st century. *J. Geophys. Res.* **120**, 784–800
739 (2015).
- 740 86. Dentener, F. *et al.* The global atmospheric environment for the next generation. *Environ.*
741 *Sci. Technol.* **40**, 3586–3594 (2006).
- 742 87. Schnell, J. L. *et al.* Effect of climate change on surface ozone over North America, Europe,
743 and East Asia. *Geophys. Res. Lett.* **43**, 3509–3518 (2016).
- 744 88. Barnes, E. A., Fiore, A. M. & Horowitz, L. W. Detection of trends in surface ozone in the
745 presence of climate variability. *J. Geophys. Res.* **121**, 6112–6129 (2016).
- 746 89. Saari, R. K., Mei, Y., Monier, E. & Garcia-Menendez, F. Effect of Health-Related

- 747 Uncertainty and Natural Variability on Health Impacts and Cobenefits of Climate Policy.
748 *Environ. Sci. Technol.* **53**, 1098–1108 (2019).
- 749 90. Yeager, S. G. *et al.* Predicting near-term changes in the earth system: A large ensemble of
750 initialized decadal prediction simulations using the community earth system model. *Bull.*
751 *Am. Meteorol. Soc.* **99**, 1867–1886 (2018).
- 752 91. Mantua, N. J., Hare, S. R., Zhang, Y., Wallace, J. M. & Francis, R. C. A Pacific Interdecadal
753 Climate Oscillation with Impacts on Salmon Production. *Bull. Am. Meteorol. Soc.* **78**,
754 1069–1079 (1997).
- 755 92. Trenberth, K. E. & Shea, D. J. Atlantic hurricanes and natural variability in 2005. *Geophys.*
756 *Res. Lett.* **33**, L12704 (2006).
- 757 93. Dai, A., Fyfe, J. C., Xie, S. P. & Dai, X. Decadal modulation of global surface temperature
758 by internal climate variability. *Nat. Clim. Chang.* **5**, 555–559 (2015).
- 759

760 **METHODS**

761
762 **Fig. 1.** Trends in annual mean temperature over 1951-2010 are calculated as an ordinary least
763 squares linear fit at each grid cell. The PDFs show the trend in spatially-averaged temperature.
764 Distributions are computed by fitting a kernel density estimate (using Matlab's 'ksdensity') to the
765 histograms of trends from each LE and from CMIP5. From CMIP5, a set of available model
766 simulations with historical and rcp85 forcing were used, ranging between one and eleven
767 ensemble members per model, totalling 123 simulations. Observations are from the Berkeley
768 Earth Surface Temperature data set⁵⁹.

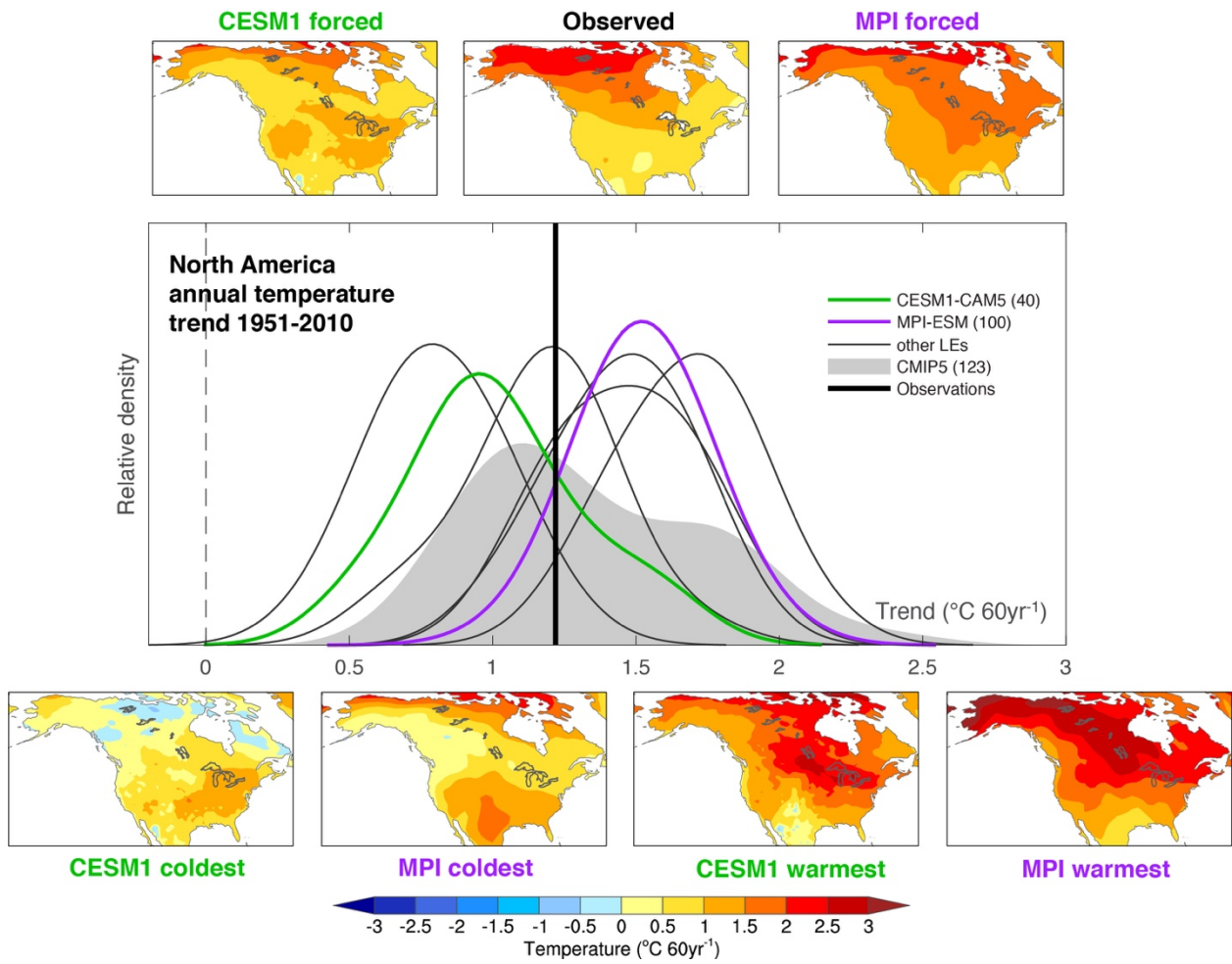
769
770 **Fig. 3.** We define a heat extreme as the 99.9th percentile of daily-mean temperatures during July
771 over the historical period 1950-1999 for each model, pooling all members of its LE for a robust
772 definition.

773
774 **Table 1.** LE initialization method. The term "micro perturbation"¹³ denotes that the LE members
775 begin from slight perturbations to a single initial atmospheric state. The term "macro
776 perturbation"¹³ denotes that the LE members begin from a variety of coupled model states (for
777 example, from different years in a long control simulation). CanESM2 consists of a hybrid
778 approach, with 10 micro ensemble members for each 5 macro ensemble members.

779
780 **The Observational LE**

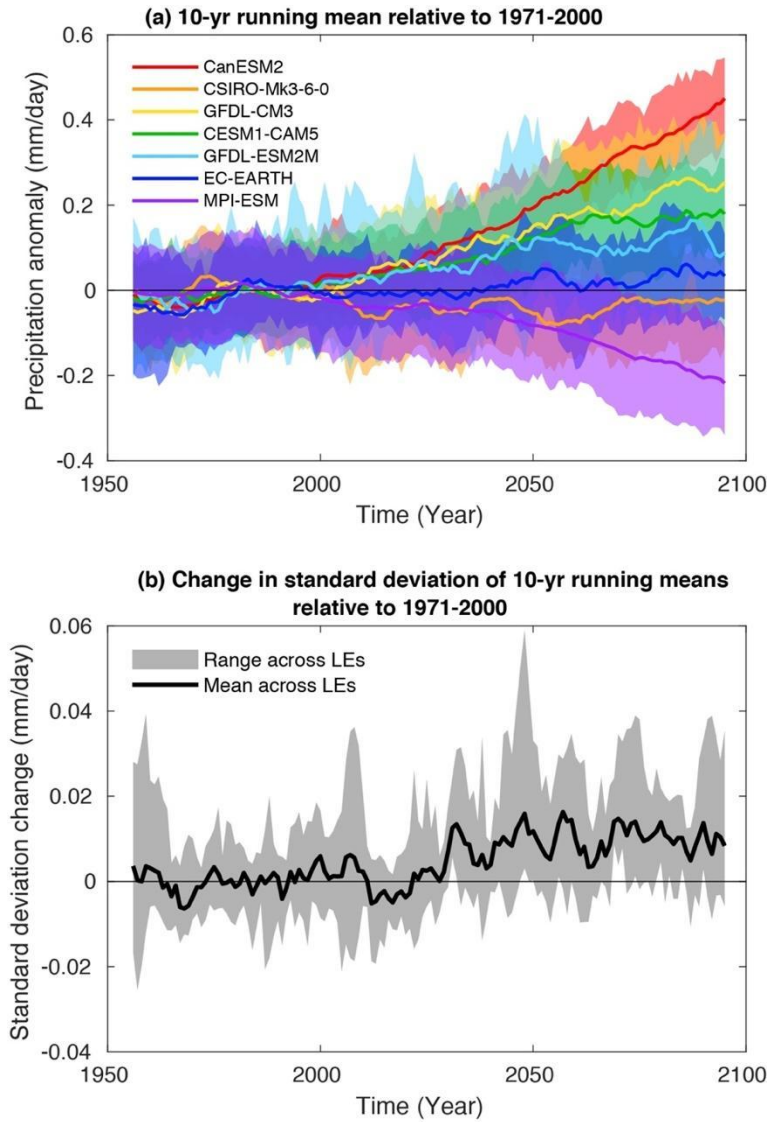
781 A brief description of the method used to construct the Observational Large Ensemble (Obs-LE)
782 is given here; further details are available in McKinnon and Deser (2018). The Obs-LE provides
783 surrogate realizations of internal variability that could have happened in the real world, while
784 largely preserving the full spatio-temporal characteristics of the actual observational record.
785 Internal variability in the Obs-LE is the sum of two pieces: a component that captures variability
786 linearly related to the three dominant ocean-atmosphere modes in the climate system (ENSO,
787 Pacific Decadal Oscillation⁹¹, and the Atlantic Multidecadal Oscillation⁹², and a component
788 termed residual "climate noise", which primarily emerges from unpredictable atmospheric
789 variability. Both pieces are estimated using monthly mean temperatures from Berkeley Earth
790 Surface Temperature (BEST) over the period 1920-2015 after an empirical removal of the forced
791 trend following ref⁹³. The spread across the ensemble is a result of the inherent randomness of
792 both the mode time series and the residual climate noise; both components contribute
793 approximately equally to the spread, although one may be more dominant than another in a
794 given location (see Fig. 8 in McKinnon and Deser, 2018). The mode-component is computed first,
795 and then subtracted from the total internal variability to obtain the residual component.
796 Specifically, the Obs-LE is created through: (1) generating new time series of the three modes
797 that share the same autocorrelation and distributions as the observed ones but have different
798 temporal phasing and multiplying them by the spatial pattern of temperature sensitivity to each
799 mode; and (2) applying a two-year block bootstrap in time to the residual climate noise
800 component. The choice of a two-year block to perform the bootstrapping provides a suitable
801 balance between accommodating any remaining temporal autocorrelation in the residual noise
802 component and number of independent samples in the record. The approach makes a key
803 assumption that the internal variability, including teleconnection patterns, of monthly

804 temperature has not changed over the period used to fit the model -- and, if used for projections,
805 will not change in the future period.
806



807
808
809
810
811
812
813
814
815
816
817
818
819

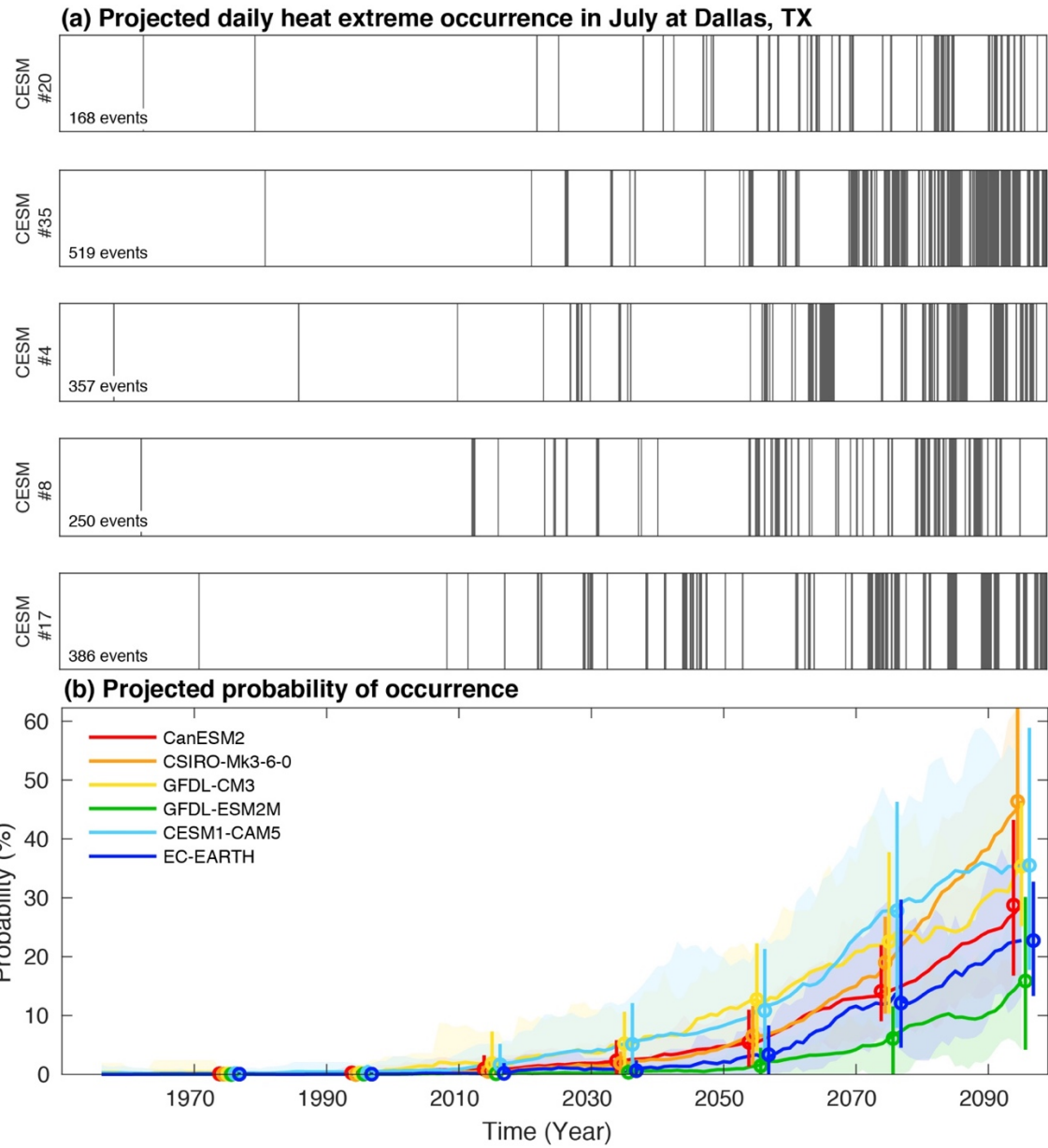
Figure 1. Internal variability and model differences in continental temperature trends. The distribution of 60-year annual temperature trends (1951-2010) over North America from 7 ESM Large Ensembles (LEs; thin curves), 40 different CMIP5 models (gray shading), and observations (Berkeley Earth Surface Temperature; vertical black line). The maps show the associated patterns of temperature trends: (top row) observed and the ensemble means (EM) from two LEs (CESM1 in green and MPI in purple); (bottom row) individual ensemble members from CESM1 (green) and MPI (purple) with the weakest ("coldest") and strongest ("warmest") trends. Note that the EM maps show the forced component of trends, while the individual member maps show the total (forced-plus-internal) trends in the model LEs. Observed trends are analogous to an individual ensemble member in that they reflect forced and internal contributions.



820
821

822 **Figure 2. Decision-making under uncertainty: Changes in mean and variability.** (a) 10-yr running
823 mean annual precipitation anomalies (mm day^{-1}) over the Upper Colorado River Basin
824 (approximated as a spatial average over $38.75\text{--}41.25^\circ\text{N}$ and $111.25\text{--}106.25^\circ\text{W}$) relative to the
825 reference period 1971-2000 from each of the 7 model LEs. Solid lines show the ensemble means,
826 and color shading the 5-95% range across ensemble members. (b) Moving average of the change
827 in standard deviation of 10-year mean precipitation (relative to 1971-2000), calculated across the
828 individual ensemble members of each model LE. The thick black curve shows the mean and gray
829 shading shows the 5-95% range across the 7 models. Note the order-of-magnitude smaller range
830 in the y-axis in (b) compared to (a).

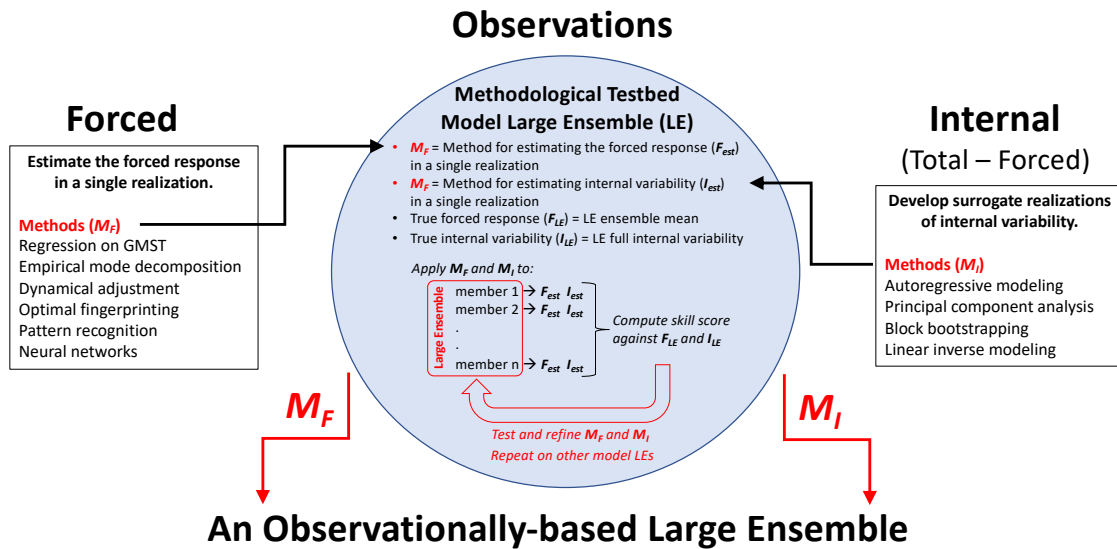
831



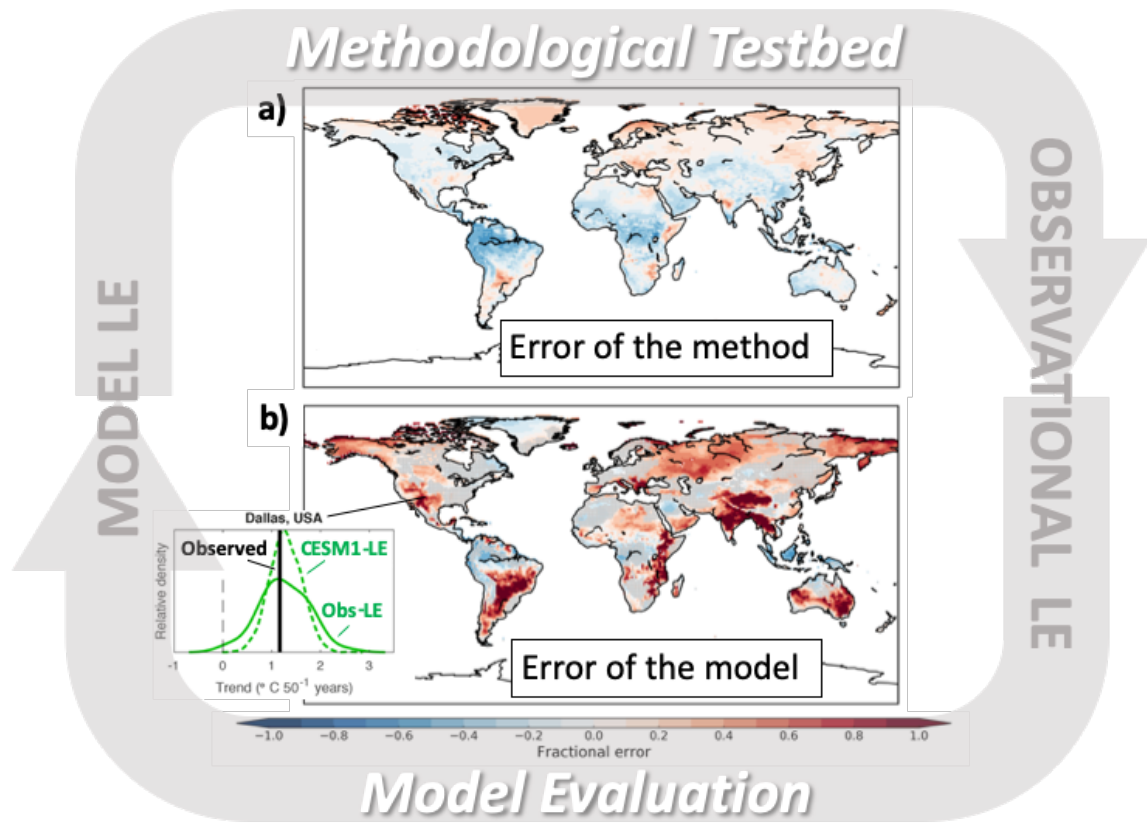
832

833

834 **Figure 3. Decision-making under uncertainty: Changes in extremes.** (a) Vertical bars mark the
 835 occurrence of July days which meet or exceed the historical (1950-1999) 99.9th temperature
 836 percentile for the grid box containing Dallas, Texas in five members of the CESM1-LE under
 837 historical and future (RCP8.5) radiative forcing. The 99.9th percentile is defined as the average of
 838 the 99.9th percentile values calculated for each ensemble member. (b) Probability of exceeding
 839 the historical (1950-1999) 99.9th percentile of daily temperature in July at Dallas, Texas for 6
 840 model LEs. Thick colored lines show the probability in each LE calculated across all ensemble
 841 members, and color shading shows the 5-95th percentile when the probability is calculated for
 842 each ensemble member separately. Open circles and vertical bars show those same values for
 843 every other decade from 1970 onwards, with models plotted in a staggered fashion centered on
 844 year 5 of a given decade. Note that the time axis shown in (b) also applies to (a).



845
 846 **Figure 4. Schematic showing the how model Large Ensembles can be used to test methods**
 847 **suitable for application to the single observational record, for example those aimed at**
 848 **separating forced climate change from internal variability.** A method (M_F) for estimating the
 849 forced response (F_{est}) can be validated using a model LE by applying it to each ensemble member
 850 individually and comparing the results to the model ensemble mean (F_{LE}) using a skill score.
 851 Similarly, a method (M_I) for developing surrogate realizations of internal variability (I_{est}) can be
 852 validated using a model LE by applying it to each ensemble member individually and comparing
 853 the results to the full range of internal variability across the model LE (I_{LE}). Various methods M_F
 854 and M_I are listed (see text for references). After validating the methods, they can be applied to
 855 the observational record to construct an observationally-based Large Ensemble (see text for
 856 details).



857
 858
 859 **Figure 5. Interplay between a Model LE and an Observational LE.** The schematic illustrates how
 860 a Model LE can be used to test the accuracy of a method for deriving surrogate realizations of
 861 internal variability based on the observational record to build an Observational LE (Obs-LE), and
 862 how an Observational LE can in turn be used to evaluate the model's simulation of internal
 863 variability. (a) The fractional difference between the spread in 50-year trends of annual near-
 864 surface air temperature in the CESM1-LE and the spread estimated from applying the
 865 methodology of McKinnon and Deser (2018) to individual members of the CESM1-LE. (b) The
 866 fractional difference between the spread of 50-year trends (1965-2014) in CESM1-LE and Obs-LE
 867 (areas in gray indicate that the difference is not significant). After McKinnon and Deser (2018).
 868 (Inset to panel b): PDFs of 50-year annual temperature trends for the grid box containing Dallas,
 869 Texas from the CESM1-LE (green; solid curve shows the model results and dashed curve shows
 870 the results based on internal variability from the Obs-LE). The vertical black bar shows the
 871 observed 1965-2014 trend value from Berkeley Earth Surface Temperature.